DETAILS OF GRAVITY DRAINAGE OF HEAVY OIL DURING VAPOUR EXTRACTION

L. James, I. Chatzis
Department of Chemical Engineering, University of Waterloo, Ontario, CANADA

This paper was prepared for presentation at the International Symposium of the Society of Core Analysts held in Abu Dhabi, UAE, 5-9 October, 2004

ABSTRACT

The recovery of heavy oil using the vapour extraction (VAPEX) process was studied in rectangular models of porous media to develop a better understanding of the gravity drainage characteristics in the vicinity of the vapour/bitumen interface. The main objective is to develop a mechanistic model for describing the evolution of the VAPEX chamber growth as a function of time and elucidate the mechanisms of VAPEX at the pore scale. Micromodels of pore networks etched on glass plates for pore scale flow visualization were used in VAPEX experiments utilising mostly butane vapour. Butane vapour was provided at constant pressure corresponding to the vapour pressure of butane at a temperature 2^{o}C lower than the temperature of micromodel with heavy oil and the vapour uptake was monitored during the experiments. It was found that the production rate of live oil depends on pore structure, the dip angle and length of the system. The evolution of the vapour/bitumen interface revealed that the pore scale aspects in VAPEX are limited to very few pores near the apparent vapour/bitumen interface. The production flow rate and sequence of pore invasion by vapour is affected by capillary phenomena that involve drainage and imbibition type displacements at the pore scale, coupled with film flow and gravity drainage near the vapour/bitumen interface. The rate of production is governed by principles of capillarity and fluid mechanics coupled with mass transfer of vapour diffusion in stagnant heavy oil and live oil at free fall gravity drainage conditions.

INTRODUCTION

Canada has the world largest reserves in heavy oil deposits (Radler, 2002). Heavy oil recovery using hydrocarbon vapour extraction (VAPEX) is an emerging new technology for in-situ recovery of heavy oil deposits. VAPEX research, over the past 10 years, has evolved from experiments with bitumen and solvent using Hele-Shaw cells (Butler, 1991; Butler 1993) to complicated experiments undertaken using porous media in various lab prototypes aimed to provide ways for up-scaling the production rate to field scale conditions (Das, 1998; Oduntan, 2001). Attempts to empirically model the VAPEX process have been moderately successful in predicting oil production rates from similar systems (Das, 1998) and applications of VAPEX process are on the pilot scale level of development. However, empirical models have failed to capture the details of VAPEX process at the pore scale. The aim of this paper is to extend the use of micromodels in VAPEX research to gain a better understanding of the pore scale events.

EXPERIMENTAL PROCEDURES

The experimental procedure followed the same methods as outlined by Chatzis (2002) with a few modifications; two water baths were used for better temperature control, the butane uptake was monitored as was the advancement of the VAPEX interface. The micromodels used had uniform pore structure as seen in Figure 1. The experimental setup for VAPEX is shown in Figure 2.

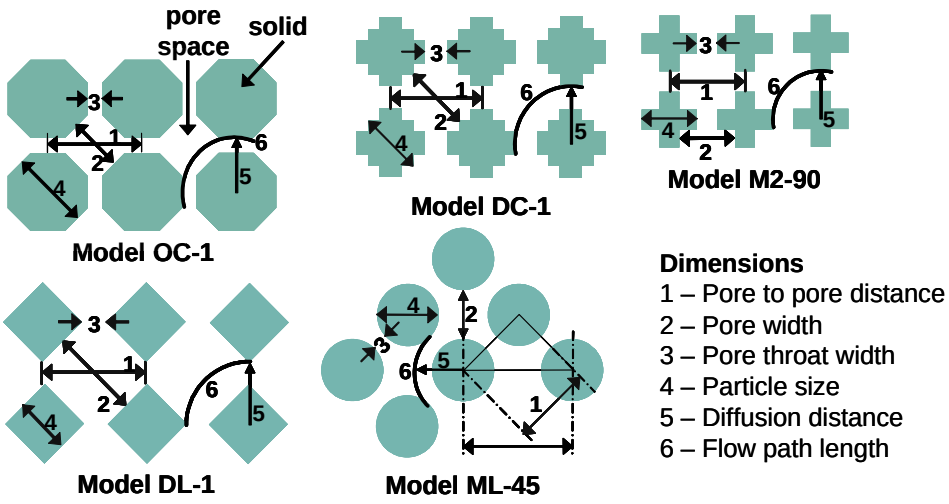

Figure 1: Micromodel Patterns used in VAPEX Experiments

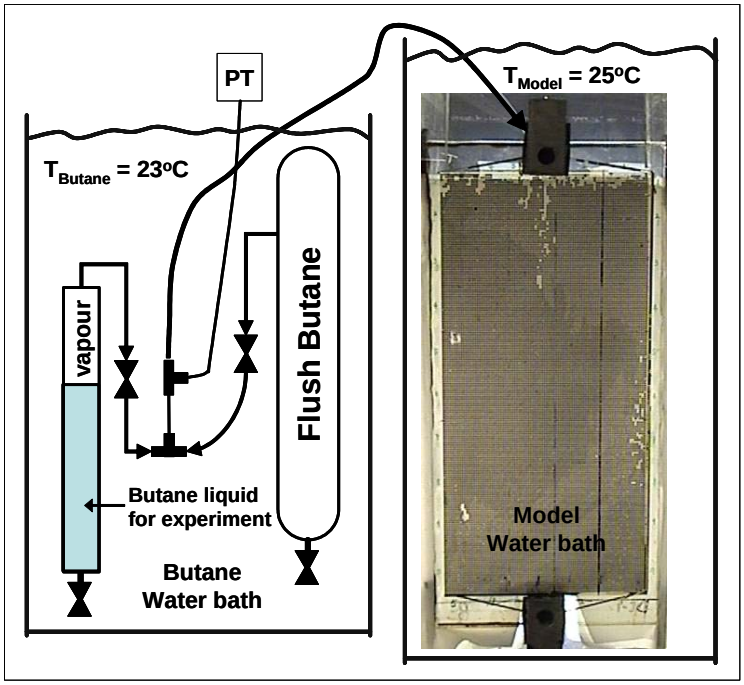

Figure 2: Experimental setup for VAPEX experiments using micromodels

During each experiment the butane vapour and the heavy oil filled micromodel were kept in separate water baths to ensure better control of their respective temperatures. Temperature control was essential to quantitatively compare results. The n-butane was maintained at 23°C and the micromodel was kept at 25°C throughout the experiment. The temperature difference ensured that the butane did not condense in the vapour chamber developed in the extracted part of the porous medium. A rectangular water bath, constructed from ½" (12 mm) Plexiglas, was used to house the micromodel. The model was then placed within two centimetres from the front of the water bath. The planar view reduced parallax and increased the clarity for image capture compared to the curved glass of a normal water bath. Water was circulated around the model for better temperature control by using an auxiliary water bath pump attached with tubing that was positioned in the 2cm gap between the model and the water bath wall. The supplied butane (Praxair instrument grade) was transferred into two different supply cylinders as shown in Fig. 2. A cathetometer was used to measure the height of butane (±0.005 cm) in the small Plexiglas cylinder ($^1/_2$" inner diameter by 12 ¾" long or 12.7 mm inner diameter by 324 mm long). A second butane cylinder (sized to fit in the water bath) was used for flushing the entire system free of air prior to starting the experiment. Flexible ¼" Tygon® tubing and a valve was attached to the production end of the model to collect the live oil.

The micromodels were divided into cell blocks using a marker to simply allow for easier position recognition within the porous network without obstructing pore visibility. They were drawn onto the front of the glass micromodel with a green colour permanent marker. Models DL-1 and OC-1 were divided into 15 horizontal rows and five vertical columns resulting in a model consisting of 75 cell blocks of 10x10 pores each except for the last rows/columns. Model DC-1 was divided into 10 rows and five columns resulting in 50 cell blocks of 20x20 pores each except for the last column and row. The VAPEX experiment started once communication between the solvent and saturated micromodel was established. As time progressed, the solvent diffused into the heavy oil, reduced its viscosity and the live oil (viscosity reduced oil) drained in the direction of gravity to the production well. The data collected during the experiment included:

- the overall trace of the position of the VAPEX interface, recording the average position of the interface (# of pores that it has advanced) for every row (vertical group of 10 or 20 pores, depending on the model) with time
- digital photographs of the overall shape of the VAPEX/bitumen interface
- digital photographs and videos capturing detailed pore scale events
- monitoring the butane uptake using a cathetometer, as indicated by the decrease in liquid butane level in butane cylinder
- monitoring the temperature in each water bath

RESULTS AND DISCUSSION

Several glass micromodels with different pore structure characteristics were used to investigate the VAPEX process in order to discern pore scale events and compare interface velocities between different models and illustrate the effect of different solvents. The micromodels are characterised in Table 1. Models OC-1 and DL-1 are comparable

except that the pore throat length in model DL-1 is negligible thus minimising the flow path. Model DC-1 has more pores that are comparable to the pore body width (dimension two) of model OC-1. However, the pore to pore distance (dimension one) and the diffusion distance (dimension five) are shorter in model DC-1. Other preliminary experiments have been conducted in unconsolidated glass micromodels using different solvents, as shown by models SUDC-2 and SUDC-3. Models M1-45 and M2-90 were used in an earlier study by Chatzis (2002). The results discussed in this paper primarily focus on results obtained using the micromodels OC-1, DC-1 and DL-1.

Table 1: Micromodel Characterisation and VAPEX Interface Rates

	Micromodels					
Remarks	**OC-1**	**DL-1**	**DC-1**	**SUDC-3**	**M1-45**	**M2-90**
C = consolidated U = unconsolidated	C	C	C	U	C	C
Length (mm/pores)	305 / 149	300 / 149	302 / 190	289 / 181	282 / 72	208 / 155
Width (mm/pores)	101 / 49	98 / 49	139 / 88	58 / 36	98 / 26	87 / 62
Dimensions (mm)						
1) Pore to pore distance	1.79	1.79	1.46	1.46	2.80	1.45
2) Pore width	1.10	1.73	1.10	1.10	2.00	1.20
3) Pore throat width	0.30	0.55	0.39	0.39	0.80	0.25
4) Particle size	1.49	1.24	1.06	1.06	2.00	1.20
5) Diffusion distance	1.04	1.16	0.93	0.92	1.80	0.85
6) Flow path length	2.32	1.83	1.82	1.82	2.83	1.59
Permeability, K (Darcy)	90	327	122	n/a	45	66
	VAPEX Interface Velocity (pores/hour)					
Location in Model	**n-butane**	**n-butane**	**n-butane**	**n-pentane**	**n-butane**	**n-butane**
41-60 pores from top	0.71	0.69	1.78	0.63		
61-80 pores from top	0.68	0.62	1.25	0.63		
101-120 pores from top	0.68	0.50	0.96	0.50		
Average (pores/hour)	**0.69**	**0.60**	**1.33**	**0.59**	n/a	**0.86**
Average (cm/hr)	**0.12**	**0.11**	**0.19**	**0.09**		**0.13**
Diffusivity (cm^2/s)	**Time to Diffuse One Pore, t_D (s)**					
1.00E-06	822.54	1030.28	653.45	650.71	2465.64	549.82
1.00E-05	82.25	103.03	65.35	65.07	246.56	54.98
2.50E-05	32.90	41.21	26.14	26.03	98.63	21.99

Once communication between the butane vapour and the bitumen saturated porous media was established, the solvent diffused into the heavy oil producing live oil and creating essentially three regions; pores with heavy (undiluted) oil, pores with live oil (with viscosity reduced) and pores filled with solvent vapour. The position of the VAPEX (oil-solvent) interface was measured with time. Some of the results are shown in Figures 3 and 4. Except for the top 10-15% of the micromodel, the VAPEX interface advanced linearly with time. The heavy oil interface was located one to two pores ahead of the measured VAPEX interface due to the fact that the live oil drained down over the pores filled with heavy oil. It should be noted that the average interface position per row (10 or 20 pores) is reported in Table 1. If the interface was not uniform throughout the row, a

weighted average was used to report the average position. In some cases, there was trapped oil left behind the interface or trapped butane at the interface, as shown in Figure 6, at time 33:15. The interface position was recorded as the furthest point of vapour phase advancement in the transverse direction.

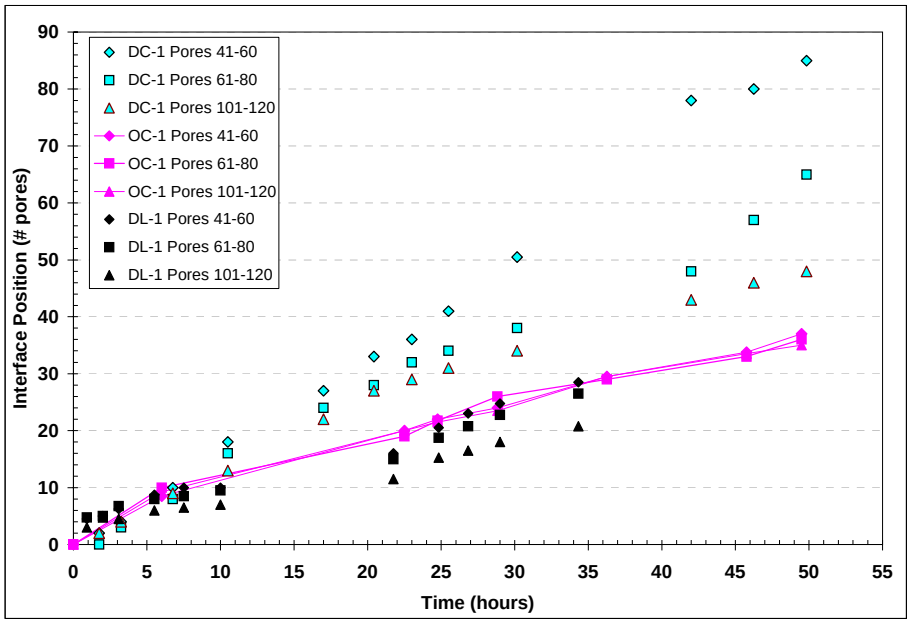

Figure 3: VAPEX Interface Advancement in Models DC-1, OC-1 and DL-1

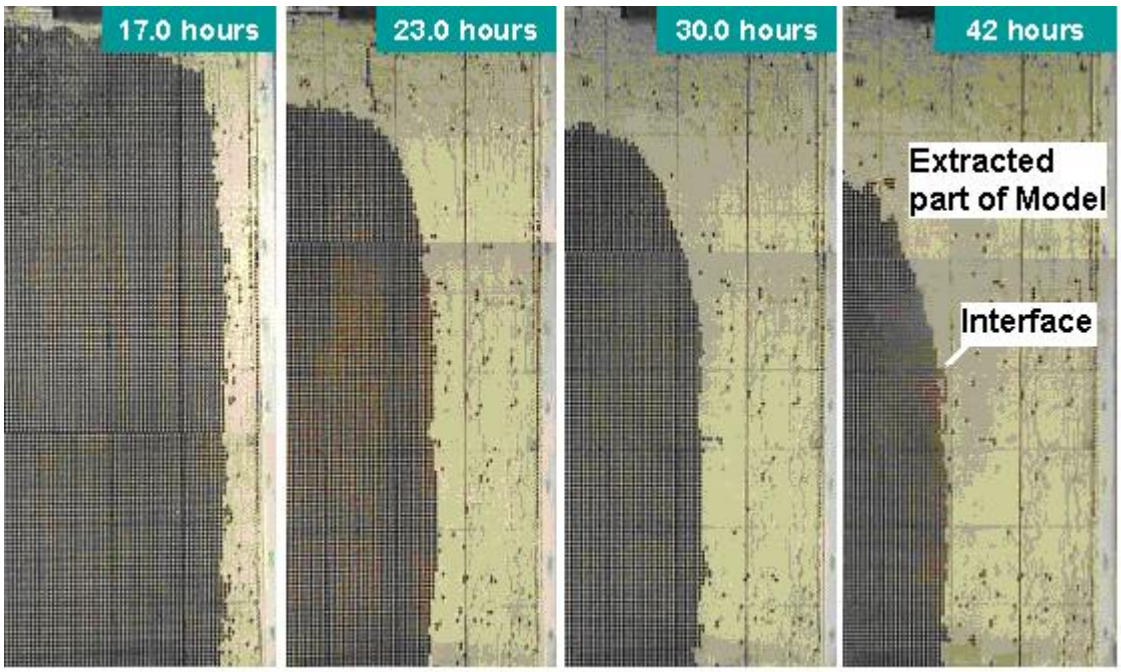

Figure 4: Change in VAPEX Interface Position with Time in Model DC-1

Figure 5 shows that the residual trapped oil was affected by the pore structure. Models DC-1 and DL-1, both with diamond shaped particles have shorter pore throat lengths compared to model OC-1. It is shown in Figure 5 that the residual oil phase for models DL-1 and DC-1 was found primarily in pore bodies sporadically throughout the model. The residual oil in model OC-1 was held preferentially in horizontally oriented pore throats, those found between vertically oriented particles or between two horizontally oriented pore bodies.

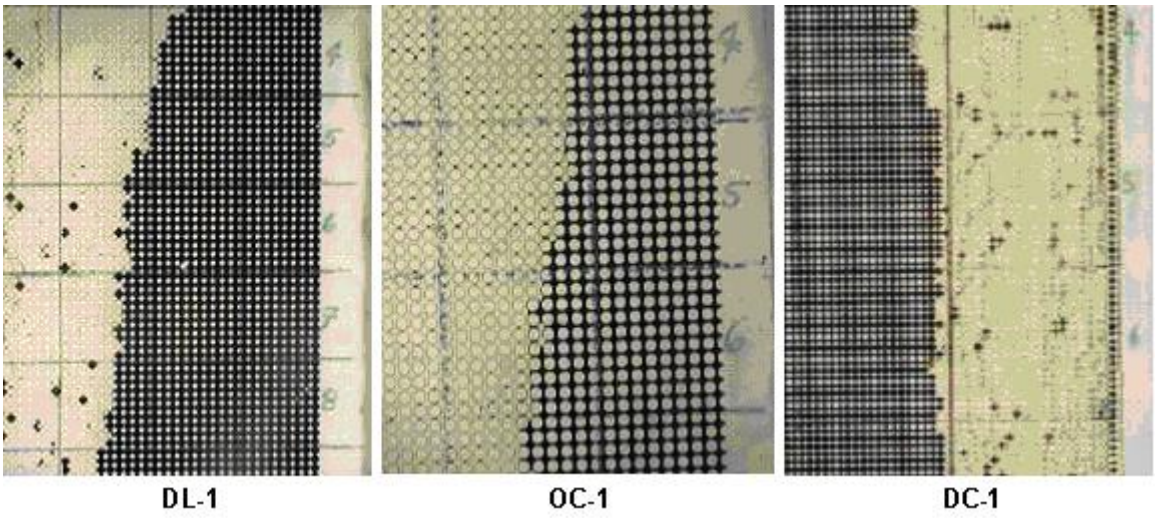

Figure 5: Residual Oil Trapped in Extracted Part in Models DL-1, OC-1 and DC-1

Figure 6 shows, in detail, how the VAPEX interface advanced in model OC-1 over a 20 minute continuous period. The time shown below each image is the time on the digital tape and it is provided for time reference. The first image shown is divided into a matrix of pores for identification. There are 18 rows (1 – 18) and five columns (a – e) of pore bodies that are referred to by their row and column numbers, i.e. pore (5, b) is in row five and column b. Also noteworthy, the pore throats are indexed using triple notation to indicate the row, column and direction (U = up, D = down, R = to the right, L = to the left). The pore throat defined as (5, b, U) is the pore throat vertically above pore body (5, b). Alternatively, the same throat could be called (4, b, D).

Image 33:15 is the first image of the series. The VAPEX interface is located in the first eight rows in the throats to the right of pores (1,b) to (8,b), i.e. (1,b,R) to (8,b,R). The interface is located in throats (9,a,R) to (13,a,R) in the next four pores. In row 14, the interface is again in the throat to the right of column b and then in rows 15-17, the interface has advanced into column c. It should be noted that the interface is in front of a peak of oil filled throats which is joined to the rest of the vapour phase by throat (15,c,L). The same pores (15,c) to (17,c) indicate that the VAPEX interface is not only solely found at the junction of pore bodies and throats. Here, it is observed that the oil phase is thicker around the solid particles to the right of pore bodies (15,c) to (17,c). This phenomenon can occur when the oil has not yet been diluted by solvent or when the live oil (diluted oil) drains in films. The image also depicts four trapped butane bubbles; a

one pore bubble in pore (5,c) and three two pore bubbles in pores (12,b)(13,b), pores (12,c)(13,c) and pores (9,c)(10,c). Images 33:52 and 34:04 show the mobilisation of live oil filling pore (12,c) and the pore throat below from the draining film along the vertical VAPEX interface. Noteworthy details in image 35:15 include the filling of pore (13,c), the size decrease of the one pore trapped butane bubble in (5,c) and the size decrease/movement of the butane bubble in (10,c) which was located in pores (9,c)(10,c).

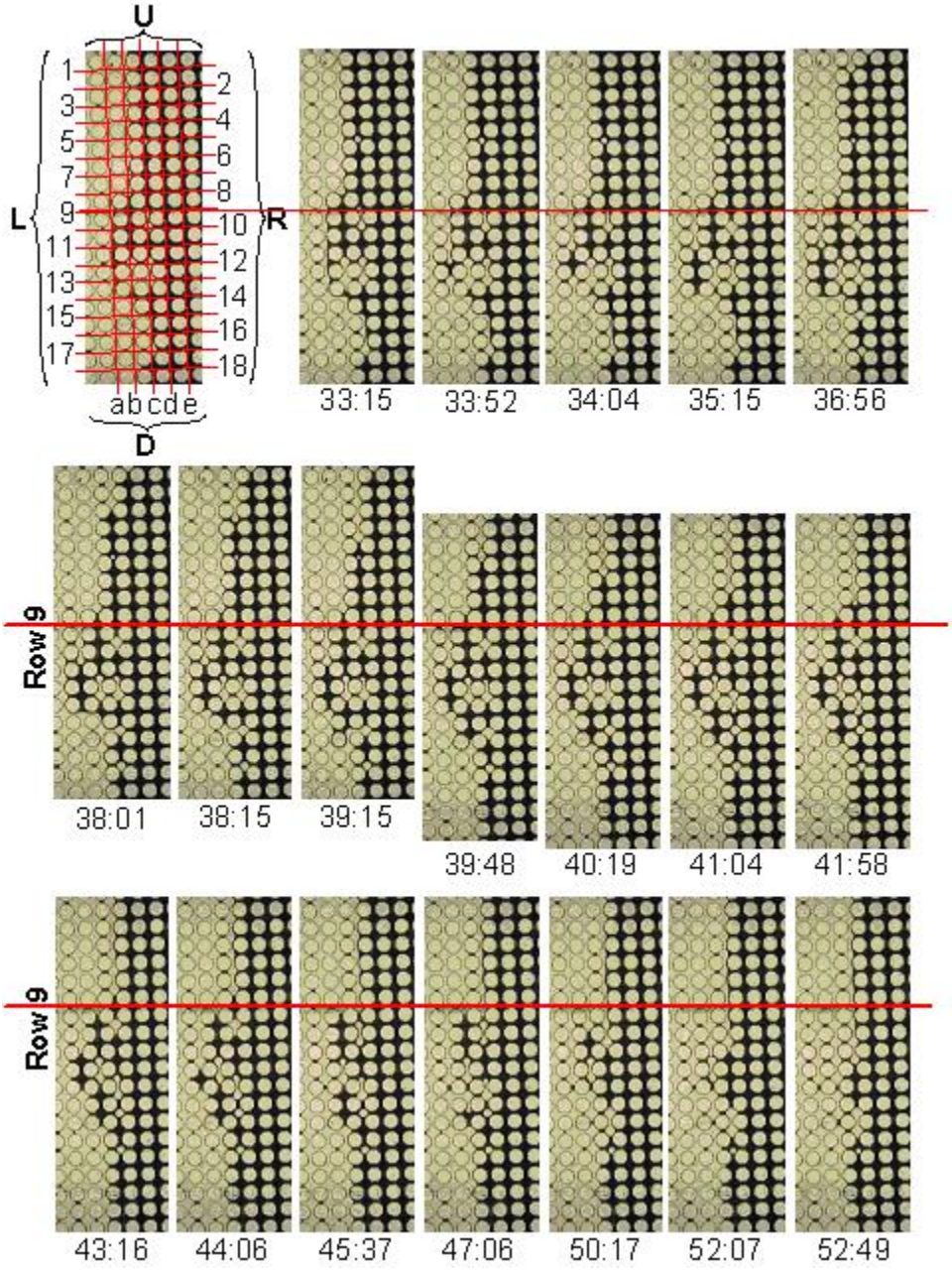

Figure 6: Pore Scale Events Illustrating VAPEX Mechanisms in Model OC-1

Trapped butane bubbles can be created by the snap-off mechanism during live oil drainage as a result of live oil flowing in pores when the trailing side of the pores contain trapped oil in pore throats, as shown in image 36:56, pore (17,c). Another example of butane trapping occurs in images 39:15 and 39:48 in pore (15,c). The trapped butane bubbles either remain stationary or are mobilized downwards in the direction of live oil drainage. During either event, the butane bubble can decrease in size due to the mass transfer of the butane from the vapour to oil phase by diffusion and convective mass transfer and/or be reconnected with the vapour phase and/or coalesce with other trapped butane bubbles if one or the other moves. The trapped vapour phase tends to remain stationary if the live oil velocity can not overcome the buoyancy forces of the bubble. While the live oil is draining in the vertical line of "c" pores, the two pore butane bubble in line "b" pores, (12,b)(13,b), remains stationary from the beginning until image 52:07 when the live oil drains from the throat above (12,b) and it reconnects with the vapour phase. It is shown through the images that the live oil is predominantly draining through the pores in line "c". Initially (image 33:15 to 39:48), there is not enough drag force from the draining oil to mobilize the butane bubble in pores (12,c)(13,c). However, it can be seen that the butane vapour in pore (12,c), the trailing pore, decreases in size throughout the same time frame. Image 40:19 shows the mobilization of the butane bubble in (13,c)(13,c,U) to image 41:04 and image 41:58 where it has resumed its two pore dimension in pores (13,c)(14,c). The trapped butane continues to be mobilised downwards in the direction of gravity and live oil drainage until the end of the captured images where it is shown at 52:49 in pores (15,c)(16,c). It should be noted that the same two pore trapped butane bubble is shown joining with a trapped one pore butane bubble in images 47:06 and 50:17. The same two images also show the two pore trapped butane bubble in pores (10,c)(11,c) reconnecting with the vapour phase via the advancement of the trailing interface downwards.

As the pore (17,c) was imbibed with live oil, the trailing live oil – butane interface advanced to (1,c). In just 15 seconds, as shown in images 38:01 and 38:15, the pore (14,b) filled with live oil and the trailing interface advanced from (1,c) at 36:56 to (2,c) at 38:01 to (3,c) at 38:15. During this downwards drainage of live oil, the trapped butane in (5,c) has become even smaller, yet it remained stationary in pore (5,c) as had the trapped butane bubbles in pores (10,c), (12,b)(13,b) and (12,c)(13,c). During the same time the trailing interface advanced to pore (5,c) where the tiny remaining butane bubble was re-introduced to the vapour phase. Overall, the trailing interface advanced from pore (1,c) at 36:56 to pore (12,c) at 52:49. In almost 16 minutes the interface advanced 11 pores. The rate of trailing pore advancement is shown in the series of images as well as in Figure 7. From frame 36:56 to 39:04, the trailing interface advanced almost one pore per minute whereas from 39:15 to 41:04 it advanced just over one and a half pores per minute. In the last 11 minutes, the advancement was less than half a pore per minute.

As shown in Table 1, the VAPEX interface advancement (V_I) in model OC-1 was 0.69 pores/hour. Using the pore to pore distance, V_I was 0.12 cm/hr. The bubble mobilization sequence shown in Figure 7 indicates that the live oil drains only in one to two pores thick region because the bubble velocity was directly related to the velocity of the

VAPEX interface advancement, V_I. The bubble velocity is indicative of the average free-fall gravity drainage pore velocity. The time for the bubble to move through one pore (1 pore / 34 seconds) predicts an overall interface velocity (V_I^*) of 0.71 pores/hour, using the following equation, where, N^v_p is the number of pores in the vertical direction, i.e. 149 pores, t_{bubble} is the time for the bubble to move one pore (34 s) and L_{model} = 30.5 cm.:

$$V_I^* = \frac{L_{model}}{t_{bubble}\ N_p^v} = \frac{L_{model}}{t_{bubble}\left(L_{model} \big/ 2.d_{pore}\right)} = \frac{2.d_{pore}}{t_{bubble}} \qquad (1)$$

While at times the bubble velocity is not constant (as seen in Figures 6 and 7), the average velocity of the draining live oil can be predicted from the rate at which the interface advances, or from knowledge of the height of the system and pore size.

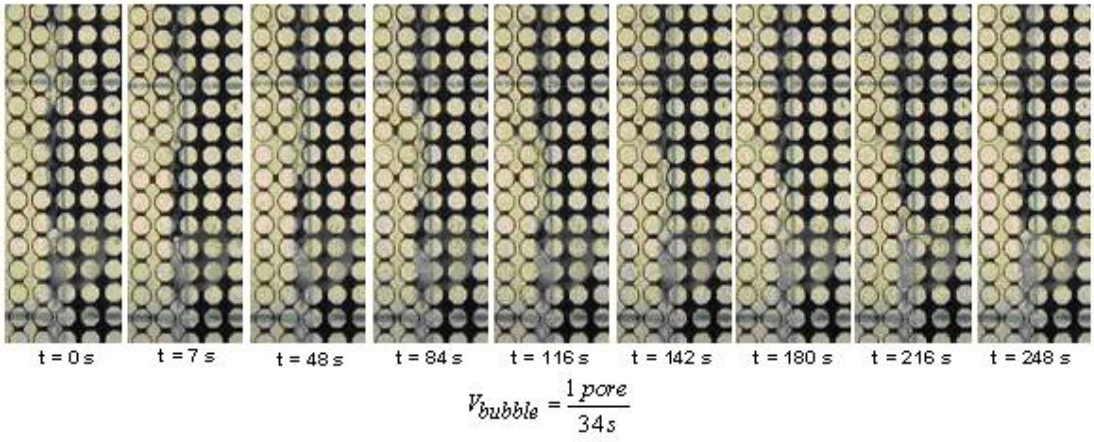

Figure 7: Mobilization of a Four Pore Bubble in Model OC-1 during VAPEX

Knowing that the live oil only flows in one to two pores, the live oil velocity (V^*_{lo}) can be predicted from the equation of Darcy flow for gravity drainage:

$$V_{lo}^* = \frac{K_{eff}\ \Delta\rho\ g}{\mu} \qquad (2)$$

where K_{eff} is the effective permeability (cm^2), $\Delta\rho$ is the difference in density between the live oil and vapour phase (g/cm^3), g is the acceleration due to gravity (981 cm/s^2) and μ is the live oil viscosity (0.05 g/cm.s). Using this information, live oil production rates can be predicted for other VAPEX experiments. The predicted (V^*_{lo}) and experimental live oil (V_{lo}) flow rates are shown in Table 2 for experiments conducted by James (2003).

It is shown that the Darcy equation of live oil flow does predict the live oil flow rate fairly reasonably especially for the consolidated models. The difference increases when comparing the predicted live oil velocity to actual live oil rates in unconsolidated media. The prediction that the live oil only flows in one pore was inferred from VAPEX experiments using glass etched micromodels that were only one pore wide with film flow

along two corners at most. In reality, the porous network is three-dimensional, where the piston-like drainage would probably still occur in one to two pores but the affect of film flow drainage is not adequately represented by the micromodel. There would be more than two corners, more likely four to six, depending on the pore shape that affect the film flow in three-dimensional porous networks.

Tables 1 and 2 also show predictions of the time to diffuse one pore (t_D) assuming a molecular diffusivity of 1E-05 and 1E-06 cm^2/s using the following equation:

$$\Delta x_{diffused} = 3.625\sqrt{D.t_D} \quad (3)$$

where Δx is the distance diffused (e.g., the diffusion distance for the micromodels and the pore diameter estimated by the particle size for the consolidated and unconsolidated media), D is the molecular diffusivity and t_D is the diffusion time. The calculation of the diffusion time for micromodel OC-1 indicated that the time to diffuse one pore (82 s using a diffusivity = 1E-05 cm^2/s) is longer than the time it takes for it to drain (on average 1 pore/34s, as shown in Table 2 and verified by the constant VAPEX interface advancement in Figure 3). However, it is also shown (Figure 6) that the live oil does not drain evenly. The pore-scale events in Figures 6 and 7 clearly indicate that convective mixing is taking place at the VAPEX interface, thus the effective diffusivity of butane (the solvent with reference to VAPEX) into the heavy oil is much greater. Using the same equation it can be inferred that an effective diffusivity on the order of 2.5E-05 cm^2/s is more realistic in terms of the rate of VAPEX interface advancement experienced in the micromodels.

Table 2: Comparison of Live Oil Velocity in Different VAPEX Systems

	Consolidated Glass Beads				Unconsolidated Troughs	
	S1	**S3**	**L2**	**L1**	**D2**	**D3**
Height, H (cm)	32.5	40.1	54.5	60.2	92	23.7
Width, W (cm)	3	4.8	4.8	4.8	0.96	0.65
Permeability, K_{eff} (Darcy)	74	68	66	76	285	350
Porosity, ϕ	0.30	0.30	0.30	0.30	0.38	0.38
Q (cm^3/min)	0.11	0.21	0.24	0.31	0.2	0.11
Q/W (cm^3/cm.min)	0.037	0.044	0.050	0.065	0.208	0.169
VAPEX Interface Velocity (cm/hr)	n/a	n/a	n/a	n/a	0.29	0.53
Live Oil Thickness, δ_f^* (mm)	0.74	0.67	0.72	0.72	0.60	0.66
Diffusivity (cm^2/s)	**Time to Diffuse One Pore, t_D (s)**					
1.00E-06	416.7	341.6	394.5	394.5	273	336
1.00E-05	41.7	34.2	39.5	39.5	27	34
Live Oil Velocity (cm/s)						
Superficial Velocity, V_{lo}	0.0083	0.0109	0.0116	0.015	0.058	0.042
Predicted Velocity, V^*_{lo}	0.0116	0.0107	0.0104	0.012	0.045	0.055
% Difference	41%	2%	10%	20%	23%	30%

* Based on experimental evidence that live oil drainage occurs in one pore, the live oil thickness was estimated as one pore diameter, approximately equal to the average particle diameter.

$$V^*_{lo} = \frac{K_{eff}\,\Delta\rho\, g}{\mu} \qquad V_{lo} = \frac{Q_{\exp}}{W\ \delta_f}$$

Constants

$\Delta\rho$ (g/cm^3)	**0.812**
g (cm/s^2)	**981**
μ (g/cm.s)	**0.05**

Production rates from consolidated and unconsolidated models with different pore scale characteristics can be compared using data shown in Table 2. The consolidated models S1 and L1 have similar permeability values and it can be seen that the live oil production rate (Q) increases with length. Models S3 and L2 demonstrate the same trend. James (2003) found that the live oil production rate increased proportionally with system's length for consolidated models while Oduntan (2001) found that the live oil flow rate in unconsolidated models of glass beads increased approximately with the square root of length, $Q \propto L^{0.55}$. The predicted velocity using Darcy's equation is comparable to the experimental superficial live oil velocity. It is assumed that the live oil viscosity in Darcy's equation is constant while in the superficial velocity calculation the live oil flow rate measured from the bottom exit of the system is divided by the effective thickness of the live oil filled pores, taken to be one pore diameter. The comparison of the two velocities calculated shows that they agree within 21% on average.

The live oil velocity calculated using Darcy's equation for free-fall gravity drainage does not depend on the length of the system for a given permeability value. Why is there an increase in live oil production rate (Q or Q/W) when the height (length) of the porous medium extracted is increased? If VAPEX experiments are performed on identical permeability systems except for the length, it is expected that the live oil production flow rate will be higher for the longer system, as shown in Table 2. Models S1, L1 and S3, L2 have similar permeability and the experiments were performed at the same butane vapour pressure with the same heavy oil, therefore the difference between them can be attributed to the length and width of the system. The two equations suggest that the live oil velocity changes with viscosity (Darcy equation) and/or film thickness (superficial velocity).

The live oil flow rate from two micromodels with same permeability could also differ with length due to the increased area for mass transfer. Two micromodels with same permeability but different lengths, L_1 and L_2, where $L_2 = 2L_1$, will have different live oil flow rates and velocities. If it is assumed that the VAPEX interface velocity (V_I) is constant and equal in both micromodels above, the live oil velocity would be same up to $L = L_1$, however, at the exit-end of the longer micromodel (L_2) the live oil velocity would be higher due to the increased area for mass transfer, i.e. WL_2 where the width (W) is the width of the porous media exposed to butane. The live oil thickness (δ_f) would likely increase towards the bottom-end of the system or the viscosity of live oil could be smaller in the longer model due to increased surface area for mass transfer. If the viscosity of the live oil (μ) is assumed to be the same in both cases, then the live oil thickness would increase with length. These aspects of VAPEX are currently under investigation.

CONCLUSIONS

There are several conclusions that can be drawn from the VAPEX experiments conducted using micromodels and slabs of consolidated and unconsolidated glass beads:

1. The rate at which the VAPEX interface advances (V_I) depends on the porous media characteristics; permeability, diffusion distance, drainage flow path, all of which depend on particle size, pore size and aspect ratio.

2. The VAPEX interface advancement is linear with time for a given cross-section. It is essentially constant over the length of the model except at the very top part of the system where the macroscopic interface is essentially flat.
3. While the draining live oil inhibits the diffusion of butane directly into the heavy oil, it also enhances mixing through pore scale events of drainage and imbibition.
4. Drainage of live oil occurs in only one to two pores at a time as shown through trapped butane bubble mobilisation. The mobilisation occurs when the velocity of the live oil overcomes the buoyancy forces of the trapped vapour. The velocity of the butane bubbles does agree with the rate of the VAPEX interface advancement.
5. The velocity of the VAPEX interface can be used to predict live oil flow rates in similar systems.

REFERENCES

1. Butler, R.M. and Mokrys, I.J., "A New Process (VAPEX) for Recovering Heavy Oils Using Hot Water and Hydrocarbon Vapour", Journal of Canadian Petroleum Technology, Vol. 30, No. 1, 1991
2. Butler, R.M. and Mokrys, I.J., "Recovery of Heavy Oils Using Vapourized Hydrocarbon Solvents: Further Development of the Vapex Process", Journal of Canadian Petroleum Technology, Vol. 32, No. 6, 1993.
3. Butler, R.M. and Mokrys, I.J., "Closed-Loop Extraction Method for the Recovery of Heavy Oils and Bitumens Underlain by Aquifers: the VAPEX Process", Journal of Canadian Petroleum Technology, Vol. 37(4), 1998.
4. Chatzis, I., "Pore Scale Mechanisms of Heavy Oil Recovery using the VAPEX Process", Proceedings of International Symposium of Society of Core Analysts, Monterey, California, September 2002.
5. Das, S.K. and Butler, R.M., "Mechanism of the Vapour Extraction Process for Heavy Oil and Bitumen", Journal of Petr. Sci. & Engineering, **21**, 43-59, 1998.
6. James, L.A., "A Closer Look at VAPEX", Masters Thesis, University of Waterloo, Waterloo, Canada, 2003.
7. Jin, W., Heavy Oil Recovery Using the VAPEX Process, Masters Thesis, University of Waterloo, Waterloo, Canada, 1999.
8. Oduntan, A.R. and Chatzis I., "Heavy Oil Recovery Using the VAPEX Process: Scale-Up Issues", Proceedings of Canadian International Petroleum Conference, Paper 2001-127, June 2001.
9. Radler, M., "Worldwide Reserves Increase as Production Holds Steady", Oil and Gas Journal, **100** (2), 113-115, December 23, 2002.